Marquette University
e-Publications@Marquette

Physics Faculty Research and Publications   Physics, Department of

Inhibition of the Aminopeptidase from *Aeromonas proteolytica* by l-leucinethiol: Kinetic and Spectroscopic Characterization of a Slow, Tight-binding Inhibitor–enzyme Complex

David L. Bienvenue
Utah State University

Brian Bennett
Marquette University, brian.bennett@marquette.edu

Richard C. Holz
Marquette University, richard.holz@marquette.edu

Marquette University

e-Publications@Marquette

Physics Faculty Research and Publications/College of Arts and Sciences

Inhibition of the aminopeptidase from *Aeromonas proteolytica* by l-leucinethiol: kinetic and spectroscopic characterization of a slow, tight-binding inhibitor–enzyme complex

David L Bienvenue
Department of Chemistry and Biochemistry, Utah State University, Logan, UT 84322-0300, USA

Brian Bennett
Department of Chemistry, Marquette University, Milwaukee, WI
Department of Chemistry and Biochemistry, Utah State University, Logan, UT 84322-0300, USA

Richard C Holz
Department of Chemistry, Marquette University, Milwaukee, WI
Department of Chemistry and Biochemistry, Utah State University, Logan, UT 84322-0300, USA

Abstract

The peptide inhibitor l-leucinethiol (LeuSH) was found to be a potent, slow-binding inhibitor of the aminopeptidase from Aeromonas proteolytica (AAP). The overall potency (K_I^*) of LeuSH was 7 nM while the corresponding alcohol l-leucinol (LeuOH) was a simple competitive inhibitor of much lower potency (K_I=17 μM).

These data suggest that the free [thiol](#) is likely involved in the formation of the E·I and E·I* complexes, presumably providing a [metal](#) [ligand](#). In order to probe the nature of the interaction of LeuSH and LeuOH with the dinuclear [active site](#) of AAP, we have recorded both the electronic [absorption](#) and EPR [spectra](#) of [CoCo(AAP)], [CoZn(AAP)], and [ZnCo(AAP)] in the presence of both inhibitors. In the presence of LeuSH, all three Co(II)-substituted AAP enzymes exhibited an absorption band centered at 295 nm, characteristic of a S→Co(II) ligand-metal charge-transfer band. In addition, absorption spectra recorded in the 450 to 700 nm region all showed changes characteristic of LeuSH and LeuOH interacting with both metal [ions](#). EPR spectra recorded at [high temperature](#) (19 K) and low power (2.5 mW) indicated that, in a given enzyme [molecule](#), LeuSH interacts weakly with one of the [metal ions](#) in the dinuclear site and that the crystallographically identified μ-OH(H) bridge, which has been shown to mediate electronic interaction of the Co(II) ions, is likely broken upon binding LeuSH. EPR spectra of [CoCo(AAP)]-LeuSH, [ZnCo(AAP)]-LeuSH, and [Co_(AAP)]-LeuSH were also recorded at lower [temperature](#) (3.5–4.0 K) and high [microwave](#) power (50–553 mW). These signals were unusual and appeared to contain, in addition to the incompletely saturated contributions from the signals characterized at 19 K, a very sharp feature at $g_{\text{eff}} \sim 6.5$ that is characteristic of thiolate-Co(II) interactions. Combination of the electronic absorption and EPR data indicates that LeuSH perturbs the electronic structure of both metal ions in the dinuclear active site of AAP. Since the spin–spin interaction seen in resting [CoCo(AAP)] is abolished upon the addition of LeuSH, it is unlikely that a μ-S(R) bridge is established.

Keywords

1. Introduction

Dinuclear metallohydrolases catalyze the degradation of many of the ubiquitous biomolecules in living organisms such as nucleic acids, phospholipids, and polypeptides [1], [2], [3], [4]. They are therefore key players in carcinogenesis, tissue repair, protein maturation, hormone level regulation, cell-cycle control, and protein degradation processes. In addition, dinuclear metallohydrolases are involved in the degradation of agricultural neurotoxins, urea, β-lactam containing antibiotics, and several phosphorus(V) materials used in chemical weaponry [5], [6], [7]. Despite their ubiquity and the considerable structural information available, little is known about how these structural motifs relate to function. The importance of understanding the mechanism of action of dinuclear hydrolytic enzymes is underscored by the recent observations that a eukaryotic dinuclear metallo-aminopeptidase is the target for the antitumor drugs ovalicin and fumagillin [8], [9]. In addition, the naturally occurring peptide analog inhibitor, bestatin, was recently shown to significantly decrease HIV infection in males by inhibiting aminopeptidase activity [10]. Thus, the inhibition of aminopeptidase activity in viruses and at malignant tumors is critically important in preventing the growth and proliferation of these types of cells and, for this reason, have become the subject of intense efforts in inhibitor design.

The aminopeptidase from *Aeromonas proteolytica* (AAP) possesses ideal properties for the study of hydrolysis reactions catalyzed by dinuclear metal centers [11]. AAP is a small, monomeric enzyme (32 kDa) that contains two g-atoms of zinc per mole of polypeptide, and is thermostable for several hours at 70 °C. AAP has been crystallographically characterized and possesses a (μ-aqua)(μ-carboxylato)dizinc(II) core with a terminal carboxylate and histidine residue coordinated to each metal ion [12]. Substitution of the two g-atoms of Zn(II) with Co(II), Cu(II), or Ni(II) provides enzymes that are hyperactive by 7.7, 6.5, and 25 times, respectively, towards certain substrates [13], [14], [15]. Moreover, Bennett and Holz [16] recently demonstrated that metal binding to AAP occurs in a sequential fashion, highlighting the potential for heterodimetallic centers. Heterodimetallic sites allows the function of each metal binding site to be studied through independent labeling with spectroscopically active and silent metal ions, respectively.

Even though thiols have been used extensively in the design of inhibitors for metalloenzyme active sites [17], [18], [19], the use of thiols as aminopeptidase inhibitors is rare [20], [21], [22]. A recent report highlighted the

slow, tight binding of peptide-thiols to AAP [23]. Based on this report, we explored the binding of l-leucinethiol (LeuSH) and l-leucinol (LeuOH) to AAP primarily because Prescott and Wilkes [11] showed that AAP has the strongest preference for substrates with a N-terminal leucine group. Analysis of both kinetic and spectroscopic data for the interaction of AAP with LeuSH at pH 7.5, have provided additional information on the interaction of thiols with the dinuclear metallo-active site of AAP.

LeuSH X = SH
LeuOH   OH
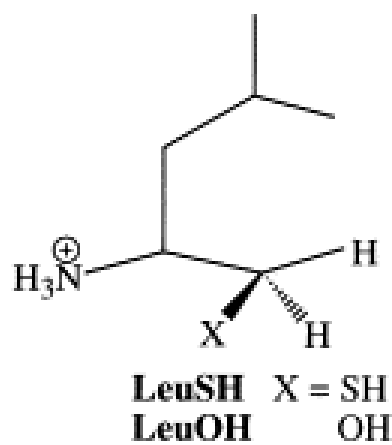
2. Materials and methods

2.1. Materials

l-Leucinethiol (LeuSH) and l-leucinol (LeuOH) were purchased from Aldrich Chemicals. Hepes buffer, l-leucyl p-nitroanilide (Leu-pNA), and $CoCl_2$ were purchased from Strem Chemicals while $ZnCl_2$ was purchased from Aldrich. Tris(2-carboxyethyl)phosphine hydrochloride (TCEP) was purchased from Boehringer Mannheim Laboratories. All other reagents used this work were purchased from either Aldrich or Sigma.

2.2. Purification of AAP

The aminopeptidase from *Aeromonas proteolytica* was purified from a stock culture kindly provided by Professor Céline Schalk [24]. Cultures were grown according to the previously published procedure [11] with minor modifications to the growth media [25]. Enzyme was purified as previously described [16], [25]. Purified enzyme was stored at −80 °C until needed.

2.3. Spectrophotometric assay of AAP

AAP activity was measured by the method of Prescott and Wilkes [11] as modified by Baker et al. [26]. In this assay, the hydrolysis of 0.5 mM Leu-pNA (in 50 mM Hepes, pH 7.5, 50 mM NaCl, 100 μM $ZnSO_4$) was measured spectrophotometrically at 25 °C by monitoring the formation of p-nitroaniline. The extent of hydrolysis was calculated by monitoring the increase in absorbance at 405 nm ($\Delta\varepsilon_{405}$ value of p-nitroaniline of 10 800 M^{-1} cm^{-1}) [27]. One unit was defined as the amount of enzyme that releases 1 μmol of p-nitroaniline at 25 °C in 60 s. The specific activity of purified AAP was typically found to be 120 units per mg of enzyme. This value is identical to that reported by Prescott and Wilkes [11]. Enzyme concentrations were determined from the absorbance at 278 nm with the value ε_{278}=41 800 M^{-1} cm^{-1} [28].

The activity of a 5 nM AAP solution was determined in the presence of 500 μM l-leu-p-nitroanilide at varying concentrations of LeuSH. The activity was measured for 10 min, during which the reaction proceeded through a non-linear phase but after ~8 min. reached a steady-state velocity indicating a slow binding process. TCEP (final concentration of 1 mM) was added to all assay reactions in order to keep LeuSH in the reduced form; this concentration of TCEP had no effect on AAP activity or stability [23]. All buffers were degassed for 30 min prior

to the addition of TCEP and kept in anaerobic vials until needed. In the presence of l-leucinol, the reaction progress curves remained linear for 10 min so initial rates were calculated from the first 60 s of the reaction. The activity of AAP was measured at five different concentrations of substrate and inhibitor. The K_I for LeuOH was obtained by fitting the kinetic data to the Michaelis–Menten equation for competitive inhibition.

2.4. Co(II)-substituted AAP samples

[CoCo(AAP)], [CoZn(AAP)] and [ZnCo(AAP)] were prepared from the purified enzyme by a method similar to that of Prescott et al. [14] and Bennett and Holz [29]. Briefly, AAP was dialyzed for 72 h at 4 °C against 10 mM 1,10-phenanthroline monohydrochloride in 50 mM Hepes buffer, pH 7.5 then exhaustively dialyzed against chelex-treated Hepes buffer. Metal insertion was effected by direct addition, with efficient mixing, of one equivalent of MCl_2 (where M=Co or Zn; ≥99.999%) followed by a 30 min incubation period at 20–25 °C. The second metal was then inserted in the same manner and the electronic absorption spectrum recorded. The inhibitor LeuSH (10 µL of a 60 mM stock solution+1 mM TCEP) was introduced directly into the enzyme sample. As in earlier work demonstrated by optical methods [30], violently flicking of the above system facilitated rapid and efficient mixing of the reagents.

2.5. Spectroscopic measurements

All spectrophotometric measurements were performed on a Shimadzu UV-3101PC spectrophotometer equipped with a constant-temperature holder and a Haake (Type 423) constant-temperature circulating bath. The use of 200 µL, 1 cm path-length microcuvettes (QS, Hellma) stoppered with rubber septa facilitated the recording of the optical spectra under anaerobic conditions. Subtraction of the absorption spectrum of apo-AAP from those of substituted enzyme samples was performed using Shimadzu UV-3101 software. Enzyme concentrations for electronic absorption studies were typically 1 mM. Low-temperature dual-mode EPR spectroscopy was carried out as in earlier work [16], [29] using a Bruker ESP-300E spectrometer equipped with an ER 4116 DM dual-mode X-band cavity and an Oxford Instruments ESR-900 helium flow cryostat. EPR spectra were recorded at a modulation frequency of 100 kHz with microwave frequencies of about 9.65 and 9.37 GHz for perpendicular and parallel modes, respectively. Precise microwave frequencies were recorded for individual spectra to ensure exact g-alignment and all spectra are presented with respect to the magnetic field range corresponding to a microwave frequency of 9.646 000 GHz. Other EPR recording parameters are specified in the figure legend. EPR simulations were carried out as in earlier work [16], [29]. All buffers for spectroscopic samples contained 20% isopropanol (v/v) to prevent aggregation at high protein concentrations. Purified enzyme stored for up to 2 weeks at 4 °C in Hepes buffer, pH 7.5, containing 20% isopropanol (v/v), showed no measurable decrease in activity. Comparison of electronic absorption and EPR spectra with those recorded in the absence of isopropanol indicated that isopropanol had no effect on the electronic structure of the dinuclear metal center [31].

3. Results

3.1. Slow-binding inhibition of AAP

Previous work indicated that thiol inhibitors of AAP act as potent, slow-binding inhibitors [23]. Upon careful examination of the hydrolysis of leucyl-*p*-nitroanilide by AAP in the presence of LeuSH in a continuous fashion, biphasic curves were observed indicative of slow-binding inhibition (Fig. 1) [32]. The kinetics of slow-binding inhibitors can be described by the following equilibria:

$$E + I \rightleftharpoons K_I E \cdot I \rightleftharpoons k_6 k_5 E \cdot I^*$$
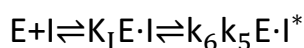
where K_I is the equilibrium inhibition constant for the formation of the initial complex, E·I, and k_5 and k_6 are the forward and reverse rate constants for the slow conversion of the initial E·I complex into a tight complex E·I*, respectively. The kinetic parameters were determined by fitting the reaction progress curves (Fig. 1) against Eq. (1):

$$Abs = v_s t + (v_o - v_s)[1 - \exp(-kt)]/k \quad (1)$$

where v_o is the initial reaction rate, v_s is the steady-state rate, and k is the first-order rate constant for the transition between v_o and v_s [33]. The parameters v_o, v_s and k were determined for each concentration of LeuSH used. Since LeuSH is a tight-binding inhibitor, it was necessary to consider the depletion of free inhibitor due to enzyme binding. Using Eq. (2) [34]:

$$I_t/(1-v_i/v_o) = E_t + [([S]+K_m)/(K_m/K_{is}+[S]/K_{ii})] \times (v_o/v_I) \quad (2)$$

it was possible to consider a decrease in the free inhibitor concentration when determining the overall inhibition constant, K_I^*, for LeuSH. In this situation v_o represents the uninhibited initial velocity, v_i is the velocity at a given concentration of inhibitor, K_{is} and K_{ii} are the inhibition constants estimated from the slope and intercept of a Lineweaver–Burke plot [35]. For competitive inhibition, K_{ii} can be considered infinite, and K_I can be substituted for K_{is}. Plotting $I_t/(1-v_i/v_o)$ versus v_o/v_i results in a straight line, the slope of which equals $K_i(1+[S]/K_m)$. Therefore, the values obtained for v_s were substituted into Eq. (2) for v_I, and plotted as a function of $I_t/(1-v_i/v_o)$ versus v_o/v_i [34], to obtain an overall inhibition constant K_I^* of 7±2 nM for LeuSH from the slope (Fig. 1). The corresponding alcohol, LeuOH, was a simple competitive inhibitor and a much less potent inhibitor than LeuSH (K_I=17±2 μM) (Fig. 2). These data suggest that the free thiol is involved in the formation of the E·I and E·I* complexes, presumably serving as a metal ligand.
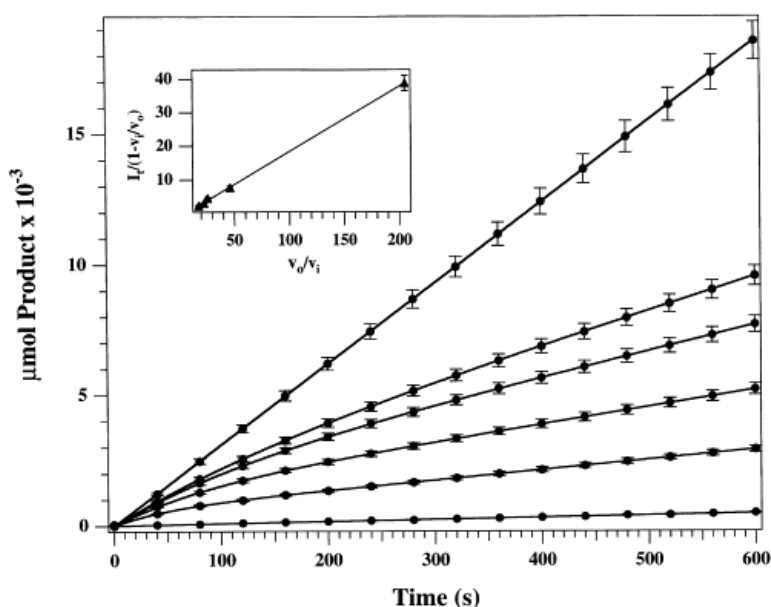

Fig. 1. Increase in absorbance at 405 nm vs. time, resulting from the hydrolysis of 500 mM l-leu-p-nitroanilide by AAP in the presence of increasing concentrations of l-leucinethiol (0.0, 10, 15, 20, 40 and 200 nM). Inset: Plot of $I_t/(1-v_i/v_o)$ vs. v_o/v_i. The parameters, v_i and v_o, obtained from fitting the kinetic data with l-leucinethiol to Eq. (1) were fit to Eq. (2) to obtain K_I=7±2 nM.
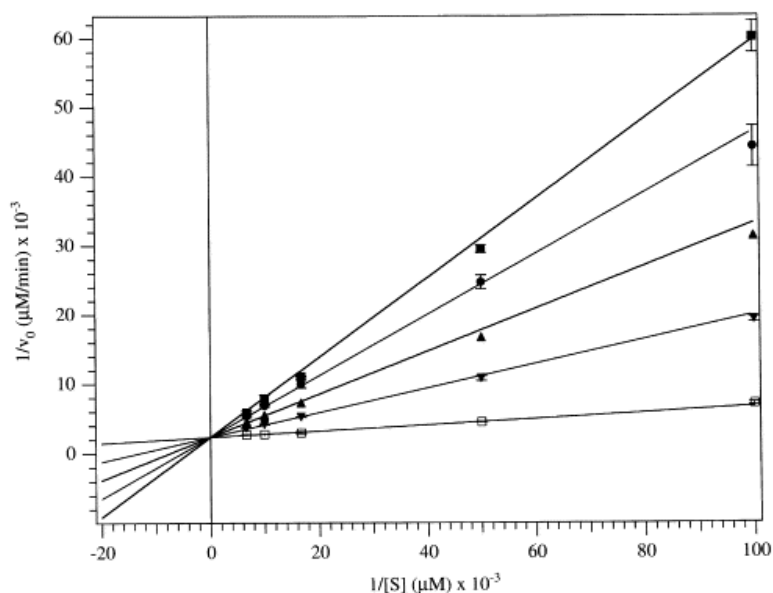
Fig. 2. Double reciprocal plot for the hydrolysis of leu-*p*-nitroanalide by AAP in the presence of increasing concentrations of l-leucinol. Assays were performed in tricine buffer, pH 8.0, 0.1 mM ZnSO₄ at 25 °C. The experimental data (symbols) were fit to the Michaelis–Menten equation for competitive inhibition. l-Leucinol concentrations were 0.0 (■), 50 (•), 100 (▲), 150 (▼) and 200 (□) μM. Error bars represent the standard deviation from the experiment performed in triplicate.

3.2. Electronic absorption spectra of LeuOH and LeuSH bound to [CoCo(AAP)], [CoZn(AAP)] and [ZnCo(AAP)]

Electronic absorption spectra of [CoCo(AAP)]-LeuSH, [CoZn(AAP)]-LeuSH, and [ZnCo(AAP)]-LeuSH were recorded in the 285 to 320 nm range (Fig. 3). All three Co(II)-substituted AAP enzymes in the presence of LeuSH resulted in an increase in the absorption band centered at 295 nm. Absorption in this region is very characteristic of a S→Co(II) ligand-metal charge-transfer (LMCT) band [36]. These absorption bands are typically observed in the 300 to 350 nm region with molar absorptivities of between 900 and 1600 M^{-1} cm^{-1} per Co(II)-thiolate interaction. As a control, a sample of Co(II)+LeuSH in 50 mM Hepes at pH 7.5 was recorded (Fig. 3, inset). These data indicate that, in the absence of enzyme, the S→Co(II) LMCT band is blue shifted to ~280 nm. Therefore, it is evident that the absorption band observed at 295 nm, in each of the AAP samples with LeuSH present, is in fact due to a Co(II)-S-thiolate interaction. Since the S→Co(II) LMCT band is observed as a weak shoulder on the $\pi-\pi^*$ protein absorption band at 280 nm, quantitation of the molar absorptivity is imprecise; however, the molar absorptivities estimated for each sample (~1900 M^{-1} cm^{-1}) are consistent with at least one Co(II)-thiolate interaction for each metal ion in the dinuclear active site.
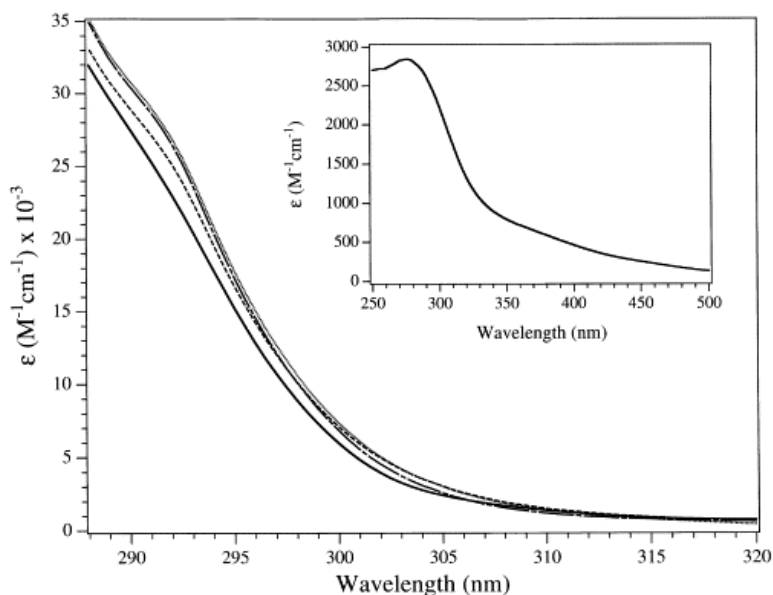
Fig. 3. Electronic absorption spectra of [ZnZn(AAP)] (solid line), [ZnCo(AAP)]-LeuSH (dashed line), [CoCo(AAP)]-LeuSH (single dashed–dotted line), [CoZn(AAP)]-LeuSH (dotted line). Inset: Co(II)+LeuSH in 50 mM Hepes, pH 7.5, in the presence of 2 equiv. of TCEP.

Electronic absorption spectra of [CoCo(AAP)], [CoZn(AAP)] and [ZnCo(AAP)] were also recorded in the 450 to 700 nm region and were identical to those previously reported for these species [14], [16], [29]. The absorption due to apo-AAP was subtracted in all cases. The absorption spectrum of [CoCo(AAP)] (Fig. 4) shows an absorption maximum of 525 nm and a molar absorptivity of ~85 M^{-1} cm^{-1}. Addition of LeuSH to [CoCo(AAP)] results in a marked change in the optical absorption spectrum (Fig. 4). There is a clear shift in λ_{max} from 525 to ~570 nm and an increase in the absorption coefficient from 85 to 230 M^{-1} cm^{-1}. Furthermore, the spectrum of [CoCo(AAP)]-LeuSH exhibits fine structure that comprises at least three absorption bands at 545, 568, and 609 nm. Similarly, the binding of LeuOH to [CoCo(AAP)] results in a red shift in the absorption spectrum from 525 to 560 nm with a concomitant increase in molar absorptivity to 145 M^{-1} cm^{-1}. Three absorption bands are also observed for [CoCo(AAP)]-LeuOH with maxima of 505, 560, and 618 nm. The increase in the absorption coefficients and the appearance of fine structure upon the binding of both LeuSH and LeuOH are indications that the electronic symmetry or coordination geometry around one or both of the Co(II) ions is significantly altered upon inhibitor binding and demonstrates the direct interaction of both LeuSH and LeuOH with the dinuclear active site of AAP.
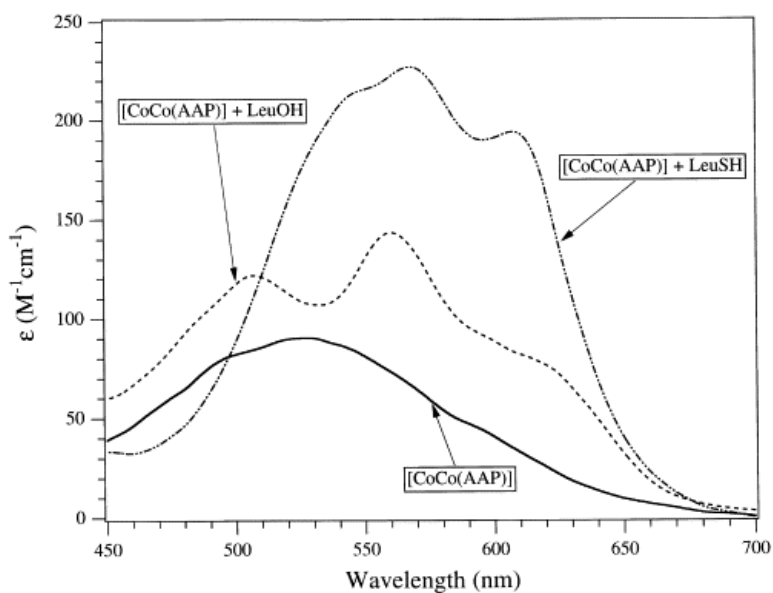
Fig. 4. Electronic absorption spectra of 1 mM [CoCo(AAP)] in 50 mM Hepes buffer at pH 7.5 in the absence (solid line) and presence of 2 equiv. of LeuSH (double dotted–dashed line) and 2 equiv. of LeuOH (dashed line). The electronic absorption spectrum of apo enzyme was subtracted in each case.

In order to ascertain the nature of the geometrical change observed for [CoCo(AAP)] upon binding LeuSH and LeuOH, electronic absorption spectra of [CoZn(AAP)] and [ZnCo(AAP)] to which either LeuSH or LeuOH was added, were recorded (Fig. 5(A, B)). The absorption coefficient of [CoCo(AAP)] (85 M^{-1} cm^{-1}) is essentially the sum of the absorption coefficients of [CoZn(AAP)] (58 M^{-1} cm^{-1}; Fig. 5(A)) and [ZnCo(AAP)] (29 M^{-1} cm^{-1}; Fig. 5(B)) and thus indicates that the individual Co(II) ions in [CoZn(AAP)] and [ZnCo(AAP)] must adopt very similar coordination geometries in their respective substituted enzyme forms as they do in the dinuclear center of [CoCo(AAP)]. The electronic absorption spectrum of [CoZn(AAP)] is consistent with the Co(II) ion in the first metal binding site adopting a distorted four- or five-coordinate geometry. The Co(II) ion in the second metal binding site likely adopts a distorted octahedral or five-coordinate geometry, based on its low molar absorptivity. Upon the addition of LeuSH to [CoZn(AAP)], the absorption coefficient more than tripled to 180 M^{-1} cm^{-1} and the λ_{max} exhibited the same characteristic red shift as that for [CoCo(AAP)] from 525 to ~570 nm (Fig. 5(A)). The spectrum also exhibits a similar fine structure pattern to that of LeuSH bound to [CoCo(AAP)]. On the other hand, the addition of LeuSH to [ZnCo(AAP)] increased λ_{max} from 525 to 555 nm with a concomitant increase in the molar absorptivity from 29 to 85 M^{-1} cm^{-1} (Fig. 5(B)). In comparison, the binding of LeuOH to [CoZn(AAP)] provides three resolvable absorption bands with a λ_{max} of 560 nm and a concomitant increase in the molar absorptivity from 29 to 60 M^{-1} cm^{-1} (Fig. 5(A)). Conversely, the addition of LeuOH to [ZnCo(AAP)] shifts λ_{max} from 525 to ~505 nm with a small increase in molar absorptivity to 50 M^{-1} cm^{-1} (Fig. 5(B)). These data indicate that the changes observed in the absorption spectrum of both [CoCo(AAP)]-LeuSH and [CoCo(AAP)]-LeuOH are dominated by the first metal binding site. Moreover, the thiolate/alkoxide moiety of LeuSH and LeuOH interacts with both of the metal ions.
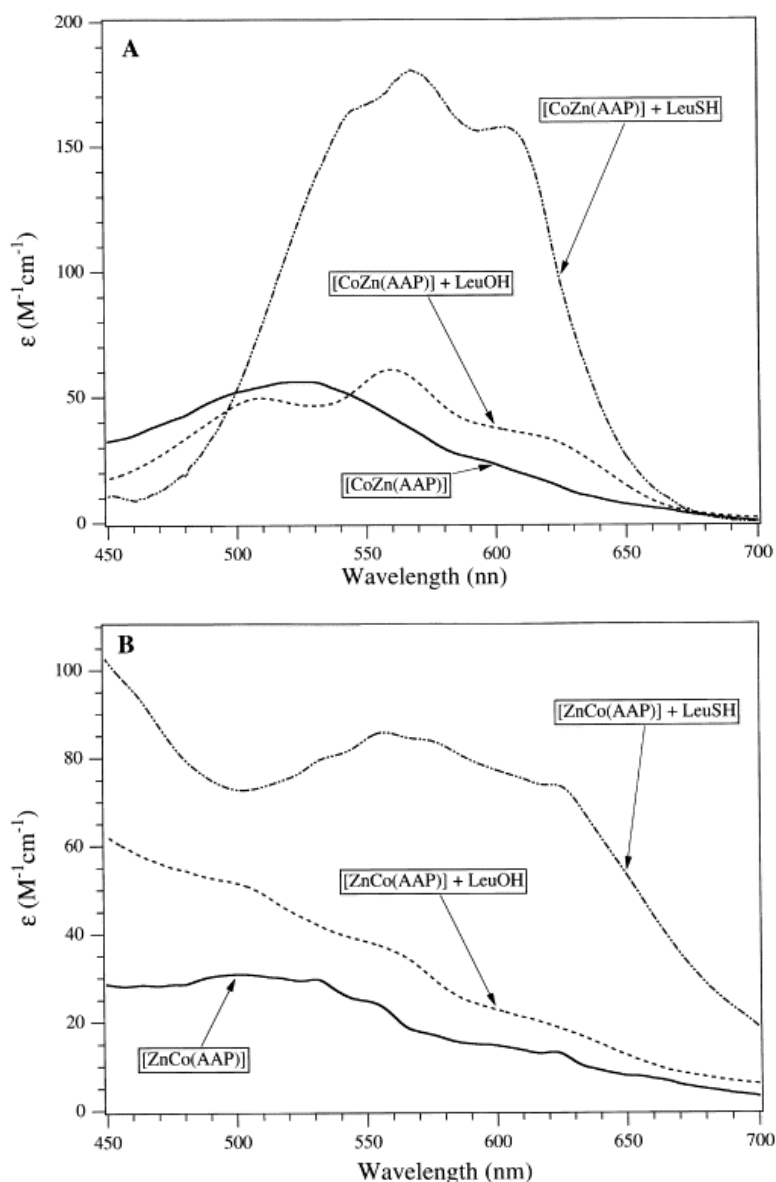
Fig. 5. Electronic absorption spectra of: (A) 1 mM [CoZn(AAP)] in 50 mM Hepes buffer at pH 7.5 in the absence (solid line) and presence of 2 equiv. of LeuSH (double dotted–dashed line) and 2 equiv. of LeuOH (dashed line); (B) 1 mM [ZnCo(AAP)] in 50 mM Hepes buffer at pH 7.5 in the absence (solid line) and presence of 2 equiv. of LeuSH (double dotted–dashed line) and 2 equiv. of LeuOH (dashed line). The electronic absorption spectrum of apo enzyme was subtracted in each case.

3.3. EPR spectra of LeuOH and LeuSH bound to [CoCo(AAP)], [CoZn(AAP)] and [ZnCo(AAP)]

EPR spectra of [Co_(AAP)], [CoCo(AAP)], [CoZn(AAP)] and [ZnCo(AAP)] have been recorded previously and are well characterized [16], [29]. EPR spectra were recorded on the various cobalt-substituted forms of AAP (i.e. [CoCo(AAP)], [ZnCo(AAP)] and [Co_(AAP)]) in the presence of excess LeuSH and LeuOH. In the case of LeuSH (Fig. 6), two distinct EPR spectra were observed depending upon the EPR running conditions. At relatively high temperatures (>19 K) and modest microwave powers (<2.5 mW), all three samples exhibited spectra indicative of a single Co(II) ion (Fig. 6(b, d, f)). However, each of the spectra actually contain two signals: (i) a featureless axial signal with $E/D \leq 0.1$ and (ii) a rhombic signal with $E/D = 0.2$–0.33 and a resolved ^{59}Co hyperfine splitting with $A_z(^{59}Co) \sim 7$ mT. The relative proportion of these signals in the spectrum of uncomplexed AAP has been shown to be pH-dependent and it was proposed that the rhombic, hyperfine split signal arises from Co(II)-OH in

[Co_(AAP)] and Co(II)-μOH-Zn(II) in [CoZn(AAP)], whereas the axial signal arises from Co(II)-OH$_2$ and Co-μOH$_2$-Zn(II), respectively [16], [29]. The observed EPR signals for [ZnCo(AAP)]-LeuSH (Fig. 6(d)) and [Co_(AAP)]-LeuSH (Fig. 6(f)) recorded at 19 K were similar to those of the uncomplexed enzyme [16], [29]. A clear hyperfine pattern was observed in the [ZnCo(AAP)]-LeuSH 19 K spectrum, with A_1(^{59}Co)=7.4 mT and centered at g_{eff}=6.61 (104 mT), compared with g_{eff}=6.88 for the resting enzyme. This pattern is part of a rhombic species with g_1=6.61 and g_2=3.09 (223 mT; cf. 214 mT for the crossover position in the spectrum of resting [ZnCo(AAP)]); the g_3 feature is broad and overlaps with g_3 of a second, essentially axial species whose $g_{perpendicular}$ feature exhibits a peak at 139 mT ($g\sim$4.96). One important difference was that the proportion of the rhombic, hyperfine split signal in the 19 K spectrum of [ZnCo(AAP)]-LeuSH was markedly greater than was seen in the resting state, indicating that a much higher proportion of the Co sites in the sample experience a constrained geometry than can be accounted for by -OH ligation as opposed to −OH$_2$.
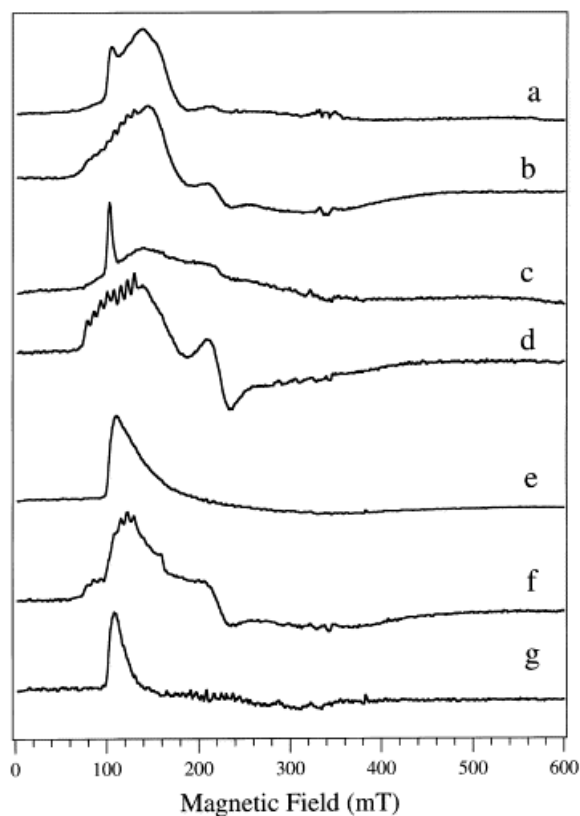

Fig. 6. EPR spectra of cobalt-substituted AAP in the presence of LeuSH: (a) [CoCo(AAP)]-LeuSH complex, recorded at 4.0 K, 50 mW microwave power; (b) [CoCo(AAP)]-LeuSH complex, 18.5 K, 2.5 mW; (c) [ZnCo(AAP)]-LeuSH complex, 4.0 K, 50 mW; (d) [ZnCo(AAP)]-LeuSH complex, 19 K, 2.5 mW; (e) [Co_(AAP)]-LeuSH complex, 4.0 K, 533 mW; (f) [Co_(AAP)]-LeuSH complex, 19 K, 2.5 mW. Trace (g) is a difference spectrum generated by subtracting the spectrum recorded at 3.7 K, 50 mW (not shown) from that recorded at 3.7 K, 553 mW (i.e. trace (e)). All samples were buffered with 50 mM Hepes buffer, pH 7.5. All spectra were recorded using 100 kHz modulation frequency, 1.26 mT modulation amplitude, 3.2 mT s^{-1} field sweep rate and 164 ms time constant.

Similarly, the 19 K spectrum (Fig. 6(f)) of [Co_(AAP)] in the presence of LeuSH shows both similarities and differences compared to the EPR spectrum of the resting enzyme ([Co_(AAP)]) [16]. The 19 K EPR spectrum of [Co_(AAP)]-LeuSH contains both a rhombic, hyperfine split signal and a featureless essentially axial signal. The rhombic species has $g_{eff\,(1,2,3)}$ values of 6.47 (at 107 mT), 3.11 (at 222 mT) and ~1.9 (at 363 mT) (cf. 6.83, 2.95, 1.96 for resting [Co_(AAP)]). This suggests a slightly lower E/D for [Co_(AAP)] in the presence of LeuSH and also an anisotropic g_{real}, as was observed for complexes of Co(II)-substituted AAP with the transition state analog inhibitor l-leucinephosphonic acid [37]. The hyperfine pattern exhibits A_1=7.1 mT, typical of signals from

magnetically isolated Co(II) in AAP. The broader signal underlying the rhombic signal exhibits a feature with a peak at $g\sim5.58$ but the signal could not be further characterized at 19 K. These data suggest that, as in [ZnCo(AAP)], LeuSH interacts with a proportion of the Co(II) ions sufficiently strongly to perturb the EPR spectrum but not sufficiently strongly to yield a single Co(II) species at 19 K or to cause dramatic changes to the EPR parameters. The mode of binding of LeuSH which causes the perturbations of the 19 K spectra of [ZnCo(AAP)] and [Co_(AAP)] therefore does not significantly affect the electronic symmetry of the Co(II) ion.

Further information about the nature of the interaction of LeuSH with AAP comes from examination of the EPR spectrum of [CoCo(AAP)] upon the addition of LeuSH, recorded at 19 K, 2.5 mW microwave power ([Fig. 6](b)). The high-temperature, low-power spectra of [ZnCo(AAP)] and [CoZn(AAP)] are clearly altered upon the addition of LeuSH, but the contributing species are similar in nature to those observed in the resting state [29]. The signal from [CoCo(AAP)], however, bears no resemblance to that of uncomplexed [CoCo(AAP)] and, instead, also resembles that of a magnetically isolated Co(II) monosubstituted species of AAP, such as [CoZn(AAP)] or [ZnCo(AAP)] [29]. The signal contains both a rhombic, hyperfine-split component, with g_1=6.56 (at 105 mT) and A_1=7.2 mT, and one or two featureless axial signals. A rhombic, hyperfine split species is not seen in resting [CoCo(AAP)] but is observed when inhibitors that break the μ-OH(H) bridge are added and when H_2O_2 is used to selectively oxidize one of the Co(II) ions to Co(III) [16], [29], [37], [38]. Thus, the implication is that the μ-OH(H) bridge is lost upon treatment of AAP with LeuSH.

EPR spectra of [CoCo(AAP)], [ZnCo(AAP)] and [Co_(AAP)] in the presence of LeuSH were also recorded at lower temperature (3.5–4.0 K) and high microwave power (50–553 mW) ([Fig. 6](a, c, e)). These signals are unusual and appear to contain, in addition to the incompletely saturated contributions from the signals characterized at 19 K, a very sharp feature at g_{eff}=6.53 ([CoCo(AAP)]-LeuSH; [Fig. 6](a)), 6.68 ([ZnCo(AAP)]-LeuSH; [Fig. 6](c)) and 6.34 ([Co_(AAP)]-LeuSH; [Fig. 6](e, g)). It is difficult to ascertain whether there are any features in the experimental spectra underlying the saturated components of the '19 K' species, and that might be associated with the $g_{eff}\sim6.5$ features. However, the difference spectrum of [Co_(AAP)]-LeuSH recorded at 553 mW and 50 mW does suggest that the $g_{eff}\sim6.5$ feature may be the only feature of the transition observable in the 0–1.05 T, 9.6 GHz EPR spectrum. These signals could be due to one of two spin states. Where a single feature at $g_{eff}\sim6$ is observed, it is often assumed that the signal corresponds to the g_1 feature of an M_s=$|\pm3/2\rangle$ transition where $E/D\sim0$. For an M_s=$|\pm3/2\rangle$ transition, as $E/D\rightarrow0$, so g_2 and $g_3\rightarrow0$, and the transition probabilities for these resonances also approach zero. Computer simulation ([Fig. 7](b)) of a species with $g_{eff(1,2,3)}$=6.68, 0.055, 0.054, corresponding to M_s=$|\pm3/2\rangle$, $g_{real}\sim2.35$ and $E/D\sim0$, provides a good model for the spectra of the cobalt-substituted AAP-LeuSH complexes. The adoption of an M_s=$|\pm3/2\rangle$ ground state implies a reversal of sign of the zero-field splitting parameter, Δ, which in turn implies a large change in the bonding organization of the Co(II) ion, consistent with direct binding of a thiol moiety to Co(II). A second possible origin of this type of spectrum exists but is not often considered. Features in the EPR spectrum, particularly the higher field (lower g) resonances, due to high-spin Co(II) ions in which the paramagnetic electron experiences a highly anisotropic coupling to the I=7/2 ^{59}Co nucleus can appear very broad, weak and asymmetric if the A tensor has only a very small projection on that particular principal g component. A model simulation ([Fig. 7](d)) was thus obtained assuming $g_{eff(1,2,3)}$=6.68, 3.1, 2.0, corresponding to M_s=$|\pm1/2\rangle$, $g_{real}\sim2.65$ and $E/D\sim0.25$, and including an anisotropic coupling $A_{(1,2,3)}$=3.0, 0.0, 1.0 mT. This model can be contrasted with one in which the electron-nuclear hyperfine interaction is isotropic and all three g factors are clearly evident ([Fig. 7](c)). The M_s=$|\pm1/2\rangle$ simulation with anisotropic $A^{I=7/2}$ (^{59}Co) reproduced the g=6.3 feature of the M_s=$|\pm3/2\rangle$ simulation. However, this simulation also produced broad, weak features at higher field. The absolute magnitudes of the principal A values were not found to be critical in the determination of the distribution of intensities of the various features in the spectrum but their relative values were important. Anisotropy of the hyperfine coupling could arise due to direct binding of a ligand atom, such as sulfur, onto which extensive electron delocalization could occur.
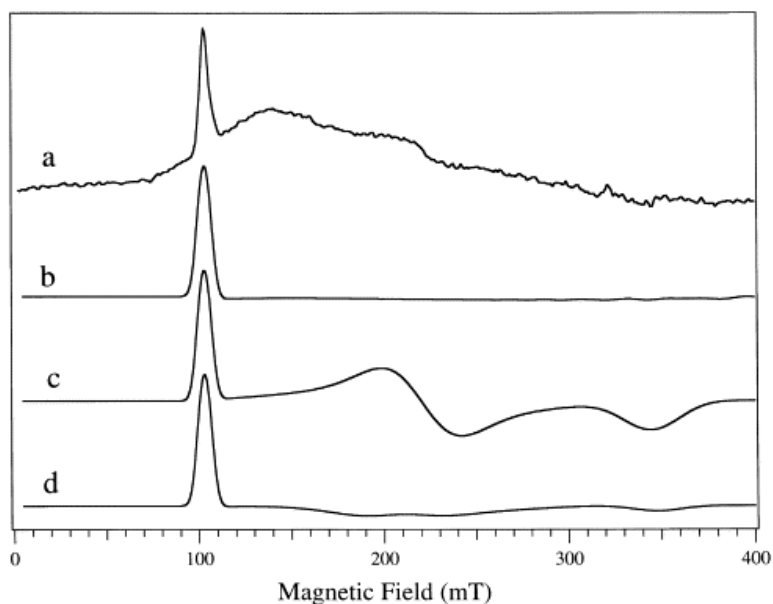
Fig. 7. Theoretical models for the origin of the $g\sim6.5$ feature in EPR spectra of AAP-LeuSH complexes: (a) EPR spectrum of [ZnCo(AAP)]-LeuSH recorded at 4 K, 50 mW. The sample was buffered with 50 mM Hepes buffer, pH 7.5. The spectrum was recorded using 100 kHz modulation frequency, 1.26 mT modulation amplitude, 3.2 mT s^{-1} field sweep rate and 164 ms time constant; (b) theoretical spectrum generated assuming $M_s=|\pm3/2\rangle$; $g_{\text{eff (1,2,3)}}$=6.68, 0.055, 0.054; $A^{l=7/2}$ (^{59}Co)=0, 0, 0 mT. Simulation assuming either isotropic or anisotropic A(^{59}Co) with a range of principal hyperfine coupling constants $A^{l=7/2}_{(1,2,3)}$ (^{59}Co)=≤3, ≤3, ≤3 mT were essentially indistinguishable; (c) theoretical spectrum generated assuming $M_s=|\pm1/2\rangle$; $g_{\text{eff (1,2,3)}}$=6.68, 3.10, 2.00; $A^{l=7/2}$ (^{59}Co)=3.0, 3.0, 3.0 mT; (d) theoretical spectrum generated assuming $M_s=|\pm1/2\rangle$; $g_{\text{eff (1,2,3)}}$=6.68, 3.10, 2.00; $A^{l=7/2}$ (^{59}Co)=3.0, 0, 1.0 mT. Linewidth and g-strain parameters were identical for the theoretical spectra (b, c, d).

Confirmation that the $g\sim6.5$ signals observed at 4 K were due to sulfur ligation to Co(II) was sought by using the analogous alcohol of LeuSH, namely, LeuOH. EPR spectra of [CoCo(AAP)]-LeuOH, [ZnCo(AAP)]-LeuOH and [Co_(AAP)]-LeuOH were recorded at ~4 K (Fig. 8(a, c, e)) and ~15 K (Fig. 8(b, d, f)). The EPR spectra of [CoCo(AAP)]-LeuOH and [ZnCo(AAP)]-LeuOH yielded novel, broad, axial EPR signals with a small (~15%) amount of a rhombic hyperfine split component as evidenced by the hyperfine pattern centered at about 105 mT, the shoulder at about 220 mT due to the derivative shaped g_2 feature, and the broad absorbance at 300 mT visible in Fig. 8(d). This signal is similar to that of resting [CoCo(AAP)] but is distinctly different from that of [ZnCo(AAP)] in the resting state. The addition of LeuOH to [Co_(AAP)] yielded spectra (Fig. 8(e, f)) with a superficial resemblance to the spectrum of resting [Co_(AAP)] at high pH [16], [29]. However, the g_2 and g_3 resonances of the LeuOH complex lie some 20 and 40 mT, respectively, downfield of those from the resting species, indicating a lower g_{real}. Thus, it is clear that LeuOH interacts with the metal ions at the active site of AAP; however, no sharp features at $g\sim6.5$ are observed.
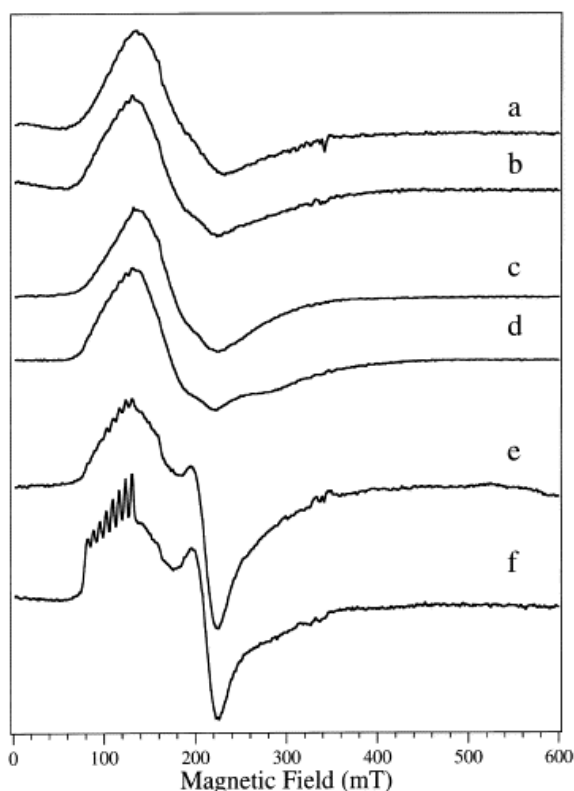
Fig. 8. EPR spectra of cobalt-substituted AAP in the presence of leucinol: (a) [CoCo(AAP)]-LeuOH complex, recorded at 3.9 K, 50 mW microwave power; (b) [CoCo(AAP)]-LeuOH complex, 14.6 K, 2.5 mW; (c) [ZnCo(AAP)]-LeuOH complex, 3.7 K, 50 mW; (d) [ZnCo(AAP)]-LeuOH complex, 14.8 K, 2.5 mW; (e) [Co_(AAP)]-LeuOH complex, 3.7 K, 533 mW; (f) [Co_(AAP)]-LeuOH complex, 16.3 K, 2.5 mW. All samples were buffered with 50 mM Hepes buffer, pH 7.5. All spectra were recorded using 100 kHz modulation frequency, 1.26 mT modulation amplitude, 3.2 mT s^{-1} field sweep rate and 164 ms time constant.

4. Discussion

Aminopeptidases are a group of exopeptidases that catalyze the hydrolysis of a wide range of N-terminal amino acid residues from proteins and polypeptide chains [39], [40], [41]. These enzymes are widely distributed in bacteria, yeast, plant, and animal tissues and, therefore, have a wide variety of biological functions such as protein maturation, protein degradation, hormone level regulation, and cell-cycle control [41]. The importance of understanding the mechanism of action of aminopeptidases is underscored by the recent observation that the naturally occurring peptide analog inhibitor, bestatin, was shown to significantly decrease HIV viral load in humans by inhibiting leucine aminopeptidase activity [10]. Because of the important physiological roles that aminopeptidases play, the design and synthesis of highly potent inhibitors for this class of enzyme that can function as potential therapeutic agents is critically important. Since thiols are known to be good ligands for Zn(II) cations [42] and Prescott and Wilkes showed that AAP has the strongest preference for substrates with an N-terminal leucine group [11], we have explored the binding of l-leucinethiol to AAP. In a previous study of peptide thiol inhibitor binding to AAP, 4-mercaptobutyrylleucyl-*p*-nitroanilide was shown to be a slow, tight-binding inhibitor with an overall inhibition constant (K_I^*) of 2.5 nM [23]. Similarly, LeuSH is an excellent inhibitor of AAP with a K_I^* of 7 nM exceeding that of the natural product bestatin (K_I=18 nM), and approaching that of amastatin (K_I=0.26 nM) and 4-mercaptobutyrylleucyl-*p*-nitroanilide (K_I=2.5 nM) [23], [43].

In order to determine how LeuSH binds to the dinuclear active site of AAP, electronic absorption spectra of the Co(II)-substituted homo- and heterometallic forms of AAP were recorded in the presence of LeuSH. Inspection of

the observed electronic absorption spectra of [CoCo(AAP)]-LeuSH, [CoZn(AAP)]-LeuSH, and [ZnCo(AAP)]-LeuSH as well as the identical complexes with LeuOH present indicates that LeuSH and LeuOH interact with both metal ions. Ligand-field theory predicts that d–d transitions of four-coordinate Co(II) complexes give rise to intense absorption ($\varepsilon > 300$ M^{-1} cm^{-1}) in the higher wavelength region of 625±50 nm owing to a comparatively smaller ligand-field stabilization energy, while transitions of octahedral Co(II) complexes have very weak absorption ($\varepsilon < 30$ M^{-1} cm^{-1}) at lower wavelengths (525+50 nm) [36]. A five-coordinate Co(II) shows intermediate features: i.e. moderate absorption intensities ($50 < \varepsilon < 250$ M^{-1} cm^{-1}) with several maxima between 525 and 625 nm [36], [44]. Upon the addition of one equivalent of LeuSH, [CoCo(AAP)], [CoZn(AAP)], and [ZnCo(AAP)] give absorption spectra that are very similar to that of the cobalt-substituted angiotensin converting enzyme in the presence of HSAc-Phe-Ala (542, 610, 634 nm, $\varepsilon \sim 350$, 520, 520 M^{-1} cm^{-1}) [45], AAP in the presence of 4-mercaptobutyrylleucyl-p-nitroanilide (570 nm, $\varepsilon \sim 270$ M^{-1} cm^{-1} with shoulders at 548, 583, and 606 nm) [23], and to those of Co(II)-substituted β-lactamases from *Bacillus cereus* and *Bacteroides fragilis* (530 nm, $\varepsilon \sim 300$ M^{-1} cm^{-1}, with shoulders at 510, 551, 610, 630 nm), which contain a Cys residue as one of the metal ligands [46], [47]. Each of these enzymes have been proposed to have five-coordinate Co(II) centers. Therefore, the Co(II) ion in [CoZn(AAP)]-LeuSH is likely five-coordinate whereas the Co(II) ion in [ZnCo(AAP)] likely resides in a penta-coordinate environment but a distorted octahedron cannot be ruled out. It is likely that distortion of each of the Co(II) ion coordination spheres is the cause of the change in electronic structure, although a change in coordination number may also be occurring. Thus, the distortion of both Co(II) ion electronic geometries from the complexation of a thiol group would be consistent with the observed optical spectral changes.

Additional structural evidence for the coordination of LeuSH to AAP was gained from EPR spectroscopy. The high-temperature, low-power EPR data from [CoCo(AAP)], [ZnCo(AAP)] and [Co_(AAP)] indicate that, in a given enzyme molecule, LeuSH interacts weakly with one of the metal ions in the dinuclear site and that the crystallographically identified μ-OH(H) bridge, which has been shown to mediate electronic interaction of the Co(II) ions [16], [29], is likely broken upon binding to LeuSH. The quite subtle changes seen in the EPR spectra of AAP-LeuSH complexes, compared to those exhibited by isolated Co(II) ions in the uncomplexed forms of the enzyme, do not suggest that the interaction which gives rise to the distorted high-temperature low-power EPR spectra involves direct binding of LeuSH via the thiol group. Binding of a single thiol group would be expected to markedly change the electronic symmetry around the Co(II) ion, except perhaps in the special case of binding in an axial position to Co(II) with very high axial symmetry. The g_{eff} values, and thus E/D, for the rhombic, hyperfine split species observed at 19 K, which have low electronic symmetry [16], [29], do not change dramatically upon adding LeuSH to AAP. Thus, it is very unlikely that these signals are due to LeuSH bound to Co(II) via –SH.

On the other hand, the EPR spectra observed at $g \sim 6.5$ for each Co(II)-substituted AAP complex of LeuSH are striking in that they bear no resemblance to any Co(II) EPR signals observed thus far from Co(II)-substituted AAP and its inhibited complexes [16], [29], [37]. The other striking feature of the observed spectra is that they are all similar to each other. This implies that reaction of LeuSH with Co(II) in either of the two sites of the dinuclear center yields electronically similar species. Such a marked change in the EPR signals from those of the Co(II) ions in uncomplexed species of Co(II)-substituted AAP is likely due to a large perturbation of the electronic structure [23]. For example, the Co(II)-substituted forms of AAP [16], *E. coli* methionyl aminopeptidase [48], *Bacteroides fragilis* β-lactamase [47], and the ribonuclease reductase R2 protein [49] all display similar featureless, i.e. axial EPR signals despite their different ligand atom quotients and geometries. Moreover, the electronic geometry of Co(II)-substituted forms bound by the transition-state analog inhibitor l-leucinephosphonic acid are not sufficiently perturbed as to result in any drastic change in the g_{eff} and g_{real} values. However, the low-temperature species observed upon the addition of LeuSH to Co(II)-substituted AAP are highly unlikely to arise as a result of an induced change in active site geometry alone. Therefore, these novel, low-temperature signals are likely the result of direct sulfur ligation of LeuSH to both Co(II) ions in the enzyme active site [23]. In support of this proposal, we have also recorded the EPR spectra of Co(II)-substituted AAP species in the presence of LeuOH and found that LeuOH does not produce this $g \sim 6.5$ signal though LeuOH does perturb the EPR signal.

Both the $M_s=|\pm 3/2\rangle$ and $M_s=|\pm 1/2\rangle$ systems described as models for the $g\sim6.5$ EPR signals likely arise as a result of direct sulfur ligation to a Co(II) ion and, thus, analysis of the EPR spectra supports our proposal that LeuSH binds to both of the metal ions via the thiol group. Since we are unable to determine unequivocally whether other features are present underneath the partially saturated '19 K' signals at 4 K, we cannot conclusively decide in favor of the $M_s=|\pm 3/2\rangle$ model over the $M_s=|\pm 1/2\rangle$ one. However, the lack of such features in the difference spectrum of [ZnCo(AAP)]-LeuSH (Fig. 7(a)) inclines us to prefer the $M_s=|\pm 3/2\rangle$ model. The observation of $g_{\mathrm{eff}}\sim6.5$ EPR signals upon LeuSH binding to Co(II)-substituted forms of AAP at low temperature and of perturbed EPR spectra at high temperature suggests that LeuSH does not discriminate between the two metal ions. This is similar to that observed for 4-mercaptobutyrylleucyl-*p*-nitroanilide binding to various Co(II)-substituted AAP enzymes [23]. Thus, it appears that LeuSH can bind to either of the metal ions through the thiol group.

Combination of the electronic absorption and EPR data indicates that LeuSH perturbs the electronic structure of both metal ions in the dinuclear active site of AAP. Moreover, these data clearly show that in a given population of enzyme, a gross change in electronic structure occurs at both metal binding sites. The EPR spectra of [CoCo(AAP)] also indicate that the Co-OH(H)-Co bridge is broken upon reaction with LeuSH. Because the electronic structure of both metal ions is altered, and because the Co-OH(H)-Co bridge is broken, it is tempting to propose that the thiol functionality of LeuSH serves to replace the μ-OH(H) bridge and binds to form a Co-S(R)-Co moiety. However, the EPR data are not consistent with such a scenario. While one of the metal ions clearly undergoes a large electronic reorganization, consistent with sulfur ligation, the remaining metal ions display electronic symmetries not unlike those of the analogous, magnetically isolated Co(II) ions in the respective uncomplexed enzyme species. In systems of low symmetry, such as [CoCo(AAP)], [CoZn(AAP)], and [ZnCo(AAP)], significant changes in the electronic properties of the $S=3/2$ high-spin Co(II) ions are predicted. The observation that one of the Co(II) ions in all of the LeuSH-complexed species of AAP studied retained an EPR signal indicative of low electronic symmetry that was only slightly perturbed from the analogous species in the respective resting enzyme, strongly argues against sulfur ligation to both divalent metal ions via a μ-S(R) bridge. In addition, the spin–spin interaction seen in resting [CoCo(AAP)] is abolished upon the addition of LeuSH and, thus, it is unlikely that a single atom bridge is retained or established. Moreover, the lack of any decrease in the [59]Co hyperfine splitting in the signals observed at high temperature (19 K) upon addition of LeuSH indicates that there is no significant electron delocalization from one of the two active site metal ions. Thus, it is not only unlikely that LeuSH provides an M-μS(R)-M bridge but, it is also unlikely that the electrophilic N-terminal amine group provides a ligand to the non-sulfur-liganded metal ion (Fig. 9), in contrast to the transition-state inhibitor l-leucinephosphonic acid [37]. Based on these data, the proposed mechanism of action for AAP can be refined [38]. Once the hydrophobic side chain is recognized by the hydrophobic pocket [31], the first binding interaction of the dinuclear cluster in AAP is carbonyl coordination to the first metal binding site, followed by N-terminal amine binding to the second metal binding site.
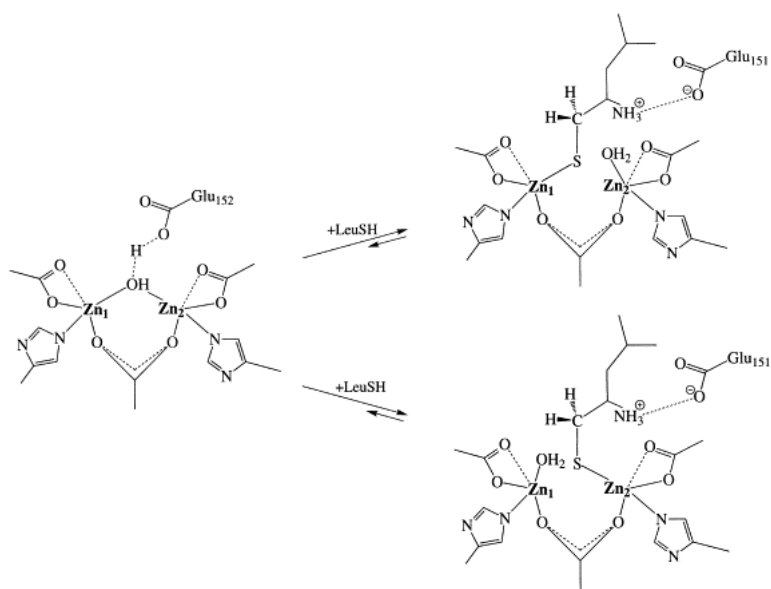
Fig. 9. Proposed mode of l-leucinethiol binding to AAP.

5. Abbreviations

AAP	aminopeptidase from *Aeromonas proteolytica*
blLAP	bovine lens leucine aminopeptidase
MAP	methionine aminopeptidase from *E. coli*
AMPP	aminopeptidase-P from *E. coli*
LeuSH	l-leucinethiol
LeuOH	l-leucinol
Hepes	[4-(2-hydroxyethyl)-1-piperazineethanesulfonic acid]
Tricine	*N*-tris[hydroxymethyl]methylglycine
LMCT	ligand-metal charge-transfer
TCEP	tris(2-carboxyethyl)phosphine, hydrochloride
Leu-*p*NA	l-leucyl-*p*-nitroanilide
EPR	electron paramagnetic resonance

Acknowledgements

References

[1] N. Sträter, W.N. Lipscomb, T. Klabunde, B. Krebs Angew. Chem., Int. Ed. Engl., 35 (1996), p. 2024

[2] W.N. Lipscomb, N. Sträter Chem. Rev., 96 (1996), p. 2375

[3] D.E. Wilcox Chem. Rev., 96 (1996), p. 2435

[4] G.C. Dismukes Chem. Rev., 96 (1996), p. 2909

[5] J. Chin Acc. Chem. Res., 24 (1991), p. 145

[6] K. Lai, K.I. Dave, J.R. Wild J. Biol. Chem., 269 (1994), p. 16579

[7] F.M. Menger, L.H. Gan, E. Johnson, D.H. Durst J. Am. Chem. Soc., 109 (1987), p. 2800

[8] N. Sin, L. Meng, M.Q. Wang, J.J. Wen, W.G. Bornmann, C.M. Crews Proc. Natl. Acad. Sci. USA, 94 (1997), p. 6099

[9] E.C. Griffith, Z. Su, B.E. Turk, S. Chen, Y.-H. Chang, Z. Wu, K. Biemann, J.O. Liu Chem. Biol., 4 (1997), p. 461

[10] G. Pulido-Cejudo, B. Conway, P. Proulx, R. Brown, C.A. Izaguirre Antivir. Res., 36 (1997), p. 167

[11] J.M. Prescott, S.H. Wilkes Methods Enzymol., 45B (1976), p. 530

[12] B. Chevrier, C. Schalk, H. D'Orchymont, J.-M. Rondeau, D. Moras, C. Tarnus Structure, 2 (1994), p. 283

[13] J.M. Prescott, F.W. Wagner, B. Holmquist, B.L. Vallee Biochem. Biophys. Res. Commun., 114 (1983), p. 646

[14] J.M. Prescott, F.W. Wagner, B. Holmquist, B.L. Vallee Biochemistry, 24 (1985), p. 5350

[15] M.E. Bayliss, J.M. Prescott Biochemistry, 25 (1986), p. 8113

[16] B. Bennett, R.C. Holz J. Am. Chem. Soc., 119 (1997), p. 1923

[17] D.W. Cushman, H.S. Cheung, E.F. Sabo, M.A. Ondetti Biochemistry, 16 (1977), p. 5484

[18] M.A. Ondetti, M.E. Condon, J. Reid, E.F. Sabo, H.S. Cheung, D.W. Cushman Biochemistry, 18 (1979), p. 1427

[19] M.M. Murphy, J.R. Schullek, E.M. Gordon, M.A. Gallop J. Am. Chem. Soc., 117 (1995), p. 7029

[20] W.W.-C. Chan Biochem. Biophys. Res. Commun., 116 (1983), p. 297

[21] E.M. Gordon, J.D. Godfrey, N.G. Delaney, M.M. Asaad, D. Von Langen, D.W. Cushman J. Med. Chem., 31 (1988), p. 2199

[22] R.E. Beattie, D.T. Elmore, C.H. Williams, D.J.S. Guthrie Biochem. J., 245 (1987), p. 285

[23] K.M. Huntington, D. Bienvenue, Y. Wei, B. Bennett, R.C. Holz, D. Pei Biochemistry, 38 (1999), p. 15587

[24] C. Schalk, J.-M. Remy, B. Chevrier, D. Moras, C. Tarnus Arch. Biochem. Biophys., 294 (1992), p. 91

[25] G. Chen, T. Edwards, V.M. D'souza, R.C. Holz Biochemistry, 36 (1997), p. 4278

[26] J.O. Baker, S.H. Wilkes, M.E. Bayliss, J.M. Prescott Biochemistry, 22 (1983), p. 2098

[27] H. Tuppy, W. Wiesbauer, E. Wintersberger Hoppe-Seyler's Z. Physiol. Chem., 329 (1962), p. 278

[28] J.M. Prescott, S.H. Wilkes, F.W. Wagner, K.J. Wilson J. Biol. Chem., 246 (1971), p. 1756

[29] B. Bennett, R.C. Holz Biochemistry, 36 (1997), p. 9837

[30] B. Bennett, B.C. Berks, S.J. Ferguson, A.J. Thomson, D.J. Richardson Eur. J. Biochem., 226 (1994), p. 789

[31] L. Ustynyuk, B. Bennett, T. Edwards, R.C. Holz Biochemistry, 38 (1999), p. 11433

[32] I.H. Segel, Enzyme Kinetics: Behavior and Analysis of Rapid Equilibrium and Steady-state Enzyme Systems, Wiley, New York, 1975.

[33] S. Cha Biochem. Pharm., 24 (1975), p. 2177

[34] J. Peter, F. Henderson Biochem. J., 127 (1972), p. 321

[35] W.W. Cleland Methods Enzymol., 63 (1979), p. 103

[36] I. Bertini, C. Luchinat Adv. Inorg. Biochem., 6 (1984), p. 71

[37] B. Bennett, R.C. Holz J. Am. Chem. Soc., 120 (1998), p. 12139

[38] C. DePaola, B. Bennett, R.C. Holz, D. Ringe, G. Petsko Biochemistry, 38 (1999), p. 9048

[39] A. Taylor FASEB J., 7 (1993), p. 290

[40] A. Taylor TIBS, 18 (1993), p. 167

[41] A. Taylor, Aminopeptidases, R.G. Landes Co., Austin, TX, USA, 1996.

[42] F.A. Cotton, G. Wilkinson, C.A. Murillo, M. Bochmann, Advanced Inorganic Chermistry, Wiley, New York, 1999.

[43] S.H. Wilkes, J.M. Prescott J. Biol. Chem., 260 (1985), p. 13154

[44] W.DeW. Horrocks Jr, B. Holmquist, J.S. Thompson J. Inorg. Chem., 12 (1980), p. 131

[45] R. Bicknell, B. Holmquist, F.S. Lee, M.T. Martin, J.F. Riordan Biochemistry, 26 (1987), p. 7291

[46] E.G. Orellano, J.E. Girardini, J.A. Cricco, E.A. Ceccarelli, A.J. Vila Biochemistry, 37 (1998), p. 10173

[47] M.W. Crowder, Z. Wang, S.L. Franklin, E.P. Zovinka, S.J. Benkovic Biochemistry, 35 (1996), p. 12126

[48] V.M. D'souza, B. Bennett, R.C. Holz, Biochemistry, in press.

[49] T.E. Elgren, L.-J. Ming, L. Que Inorg. Chem., 33 (1994), p. 891